J. Opt. A: Pure Appl. Opt. **2** (2000) 272–278. Printed in the UK PII: S1464-4258(00)10386-1

Characterization of azobenzene chromophores for reversible optical data storage: molecular quantum calculations

Thomas G Pedersen†, Per M Johansen‡ and Henrik C Pedersen‡

† Institute of Physics, Aalborg University, Pontoppidanstræde 103, DK-9220 Aalborg East, Denmark
‡ Department of Optics and Fluid Dynamics, Risø National Laboratory, DK-4000, Denmark

Received 14 December 1999, in final form 27 January 2000

Abstract. Azobenzene chromophores are promising as molecularly engineered materials for reversible optical data storage based on molecular reorientation. In this paper, the optical properties of several different azobenzene chromophores are studied using molecular quantum calculations. Special emphasis is put on molecular anisotropy since a high degree of anisotropy is essential for the storage performance. The *trans* isomers are all found to be practically one-dimensional whereas the anisotropy of the *cis* isomers is highly dependent on substituents. Molecular reorientation of chromophores in liquid-crystalline polymers is simulated in order to study the influence of lacking *cis* anisotropy. It is demonstrated that photoinduced birefringence is significantly reduced in materials characterized by a low degree of *cis* anisotropy.

Keywords: Azobenzene, optical data storage, quantum calculations

1. Introduction

Optical data storage in organic as well as inorganic materials relies on the possibility of altering the refractive index of the material by means of light. In addition, the storage process can be made reversible provided data can be erased by light or heating and in this case the storage medium can be reused several times. This highly desirable property is found in many azobenzene compounds [1–7]. Information is stored in these organic materials by linearly polarized laser beams encoded with the data. Furthermore, data storage and retrieval can be either serial or parallel by utilizing focused single beams or holographic setups [7], respectively. In order to obtain high storage rates the wavelength of the writing beam must coincide with an absorption band of the material. Conversely, data retrieval without erasure is ensured by applying a read-out wavelength, which lies well outside the absorption band. Whenever desired, however, data can be erased in a controllable fashion by exposure to UV radiation [8] or simply by changing the polarization of the writing beam from linear to circular [9]. Once it has been written, the modulation of the refractive index should be prevented from decaying significantly before the time of data retrieval or erasure. Hence, material stability is an important issue and various ways of freezing the index modulation have been realized. By attaching the azobenzene chromophores to amorphous high T_g (glass transition temperature) polymers, Natansohn *et al* [3,4] have produced materials with excellent long-term stability. Alternatively, Hvilsted *et al* [5,6] have demonstrated stability of several years in liquid-crystalline polymers containing azobenzene side-chain units.

The basic storage mechanism in azobenzene compounds is now reasonably well understood. The azobenzene molecule exists in two distinct structural forms: rod-like *(trans)* and bent *(cis)* and as the *trans* isomer is the thermally stable one, the material is initially in an all-*trans* state. Photons are absorbed by illuminating the material in the *trans* absorption band and with a certain probability (quantum efficiency) the absorption event is followed by $trans \rightarrow cis$ isomerization, i.e. a change of the molecular structure. Provided the writing wavelength coincides with the *cis* absorption band as well, repeated $trans \rightarrow cis \rightarrow trans$ cycles will be induced. The polarizabilities of *trans* and *cis* chromophores are different and hence a spatially varying *cis* population leads in itself to a modulation of the refractive index. However, since the *cis* isomer is thermally unstable this effect is not useful for long-term storage applications. Instead, permanent storage is attained through index changes induced by optical reorientation of the chromophores [2–7]. Optical reorientation is believed to occur as a result of the angular selectivity of absorption events. In a sample containing perfectly anisotropic chromophores, light is primarily absorbed by molecules with the transition dipole moment parallel to the polarization

1464-4258/00/040272+07$30.00

of the optical beam. During isomerization, the enhanced mobility of the excited chromophore allows the molecule to reorient itself. In amorphous polymers, the reorientation is adequately modelled as being essentially random [10]. Conversely, following the mean-field picture presented by the present authors [11, 12] the excited molecules in liquid-crystalline polymers tend to rotate towards the nematic director. In the case of amorphous polymers, a particular chromophore is repeatedly excited until it, by chance, ends up oriented perpendicular to the optical field since in this case light can no longer be absorbed by the molecule. Thus, prolonged illumination produces a state in which the majority of chromophores are located in the plane perpendicular to the polarization of the incident beam. In the liquid-crystalline case, the angular distribution of molecules in a particular microdomain is initially symmetric around the domain director. However, by angularly selective absorption the angular distribution is depleted of those molecules that are approximately parallel to the field. Subsequently, the enhanced mobility allows these molecules to lower the energy by rotating towards the domain director [11, 12]. This, in effect, tilts the domain, and in the process of re-establishing the equilibrium distribution the director rotates outward from the polarization direction. Hence, prolonged illumination produces a state in which the entire *domains* have been reoriented into the plane perpendicular to the field. The rotation *away* from the polarization direction has been clearly confirmed experimentally [2–7] and serves to distinguish the effect from, for example, optical reorientation in ordinary dye-doped liquid crystals [13].

Obviously, the storage performance of both amorphous and liquid-crystalline azobenzene polymers is determined by macroscopic as well as microscopic parameters. By macroscopic we understand parameters that are properties of the entire sample, e.g. phase behaviour and alignment potential in the liquid-crystalline case. These properties are essential for the stability of the material. Conversely, the microscopic parameters count the properties of the individual chromophores, i.e. absorption cross section, polarizability, dipole moment and quantum efficiency, that can be manipulated chemically by attaching substituents to the azobenzene molecule. These parameters govern several crucial aspects of the storage performance. First, the rate of $trans \rightarrow cis \rightarrow trans$ cycles and thereby the storage rate is determined by the *trans* and *cis* absorption cross sections in conjunction with the $trans \rightarrow cis$ and $cis \rightarrow trans$ quantum efficiencies. Second, as explained above, optical reorientation relies on angular selectivity of absorption events and therefore the absorption anisotropy of the chromophores is an important parameter. Third, the refractive index modulation accompanying optical reorientation is determined by the molecular polarizability tensor at the read-out wavelength. Clearly, a large index modulation requires a highly anisotropic polarizability.

From the nature of the storage mechanism it follows that improved storage performance can be achieved by increasing absorption cross sections, quantum efficiencies and the molecular anisotropy. However, to retain a reasonable optical penetration depth the absorption cross sections cannot be allowed to increase beyond a certain limit. Increased

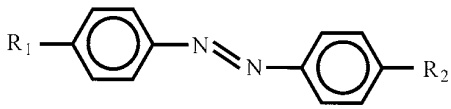

Comp #	R_1	R_2
1	MeO	C≡N
2	MeO	NO_2
3	N-Me_2	O H-C
4	N-Et_2	NO_2

Figure 1. Chemical structure of the azocompounds.

$trans \rightarrow cis$ and $cis \rightarrow trans$ quantum efficiencies would generally improve the storage performance. These quantities are known, however, to be rather insensitive to the choice of substituents [14]. This leaves the molecular anisotropy as the obvious parameter for optimization of the microscopic properties. It is the purpose of this paper to study theoretically the influence of substituents on the storage performance of azobenzene chromophores. We present results of quantum chemical calculations of the absorption cross section, absorption anisotropy, polarizability and polarizability anisotropy. The particular chromophores shown in figure 1 are selected because the fundamental *trans* $\pi \rightarrow \pi^*$ absorption maximum of these molecules increases gradually from ultraviolet (360 nm) in compound #1 to green (500 nm) in compound #4. Hence, by comparison it is possible to correlate the storage performance with the absorption maximum. Furthermore, we present simulations of the influence of varying molecular anisotropy on the intensity-dependent photostationary birefringence.

2. Quantum chemical model and results

The quantum calculations are based on a previously formulated extended Pariser–Parr–Pople (PPP) model which includes nonbonding states in a perturbative manner [15]. The PPP model in itself usually gives an accurate description of the location and intensity of the strong $\pi \rightarrow \pi^*$ transitions which dominate the spectra of both *trans* and *cis* isomers. However, with azocompounds in which the fundamental $\pi \rightarrow \pi^*$ transition is in the UV, there normally exists a separate $n \rightarrow \pi^*$ absorption band (n: nonbonding) which dominates the optical properties in the corresponding wavelength range. In azocompounds with a low-lying $\pi \rightarrow \pi^*$ transition (so-called pseudo-stilbenes according to Rau's classification [14]), the two types of absorption bands coincide. Since the intensity of $n \rightarrow \pi^*$ band is generally weak, transitions involving nonbonding states can be neglected in this case. Experimental *trans* absorption spectra for compounds #1 [6] and #2 [16] show that these display pronounced $n \rightarrow \pi^*$ bands. The calculations presented here indicate that compounds #3 and #4 belong to the pseudo-stilbene group. The geometries of *trans* and *cis* isomers are shown in figure 2. An important point is that both isomers are non-planar, i.e. have a non-vanishing twist angle τ. It is the presence of twisted bonds which makes the $n \rightarrow$

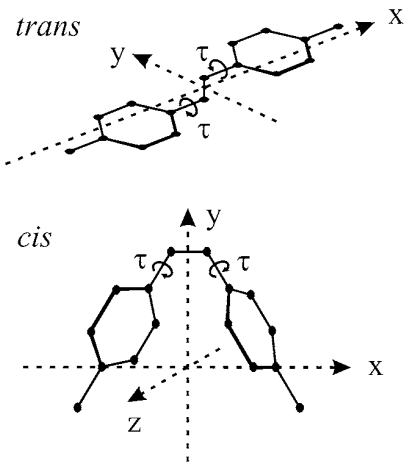

Figure 2. Geometry of *trans* and *cis* isomers. Twisted bonds are indicated by the twist angle τ.

π^* transition allowed since the n- and π^*-orbital axes would be perpendicular in a planar geometry. For all compounds the twist angles are taken as those obtained in [15], i.e. $\tau = 20^\circ$ for the *trans* isomer and $\tau \approx 50^\circ$ for the *cis* isomer. All parameters entering the quantum calculations (resonance integrals, one-centre integrals, ionization potentials and bond lengths) are standard values taken from [17] supplemented by parameters for O in nitro groups [18] and for simplicity the ionization potentials of the NMe_2 and NEt_2 groups are taken as that of N. Non-zero twist angles are incorporated into the PPP model, which was originally formulated for planar systems, by modifying the resonance integrals according to $\beta(\tau) = \beta_{\pi\pi}\cos(\tau)$ and $\beta(\tau) = \beta_{\pi n}\sin(\tau)$ for π–π bonds and π–n bonds, respectively [15,17]. The computer code has been developed by the authors and configuration interaction is incorporated at the singly excited state level. The relatively simple PPP scheme is not sufficiently reliable to be used for geometry optimization. Hence, we neglect any substituent dependence of the twist angles. Since there is no steric hindrance for a planar geometry of *trans* isomers these may, in fact, be less twisted than assumed above. The degree of molecular anisotropy is expected to decrease as the twist angles are increased due to coupling between orbitals in the (x, y) plane and orbitals directed along z; see figure 2. Hence, the deviations from perfect anisotropy calculated using $\tau = 20^\circ$ can be viewed as upper values. It is found below, however, that all *trans* isomers remain practically one-dimensional even with $\tau = 20^\circ$. It follows that conclusions regarding the optical properties of the *trans* isomers remain valid even if the assumed τ-value is too high.

In order to describe the anisotropy of the molecules we need to compare the Cartesian components of absorption cross section and polarizability. Hence, the absorption cross section of a molecule illuminated by light polarized along the molecular x-direction is denoted σ_x etc, and similarly α_{xx} denotes the xx-component of the polarizability in the molecular coordinate system. All optical constants are obtained using the procedure presented in [15] which includes a Gaussian broadening of the transitions. The optical properties of the chromophores are given with reference to the coordinate systems shown in figure 2. The axes are chosen so as to coincide as nearly as possible with the principal axes of the molecules. In practice, this is done by using coordinate systems in which the transition dipole moment of the fundamental $\pi \rightarrow \pi^*$ transition coincides with the x-axis. In this manner, a perfectly anisotropic molecule is one for which σ_x and α_{xx} are the only non-vanishing components of absorption cross section and polarizability. Note that different coordinate systems are used for different molecules and also for different isomers of the same molecule.

Some of the characteristics of the four azo chromophores are listed in table 1. The position of the fundamental $\pi \rightarrow \pi^*$ transition is given by the singlet energy E_S. For the *trans* isomers this quantity is seen to decrease from 3.41 to 2.48 eV corresponding to a shift in the wavelength of maximum absorption from 363 to 500 nm. The shift is mainly attributed to increased polarity as seen from the corresponding dipole moments. Also, the oscillator strength of the $\pi \rightarrow \pi^*$ band increases from compound #1 through #4. Finally, the energy of the lowest triplet E_T shows a decreasing tendency with polarity in correspondence with the singlet energy. For the *cis* isomers, E_S and E_T show a similar tendency. In this case, however, the oscillator strength does not follow a simple pattern. The generally large polarity of all *trans* isomers agree with the ability to form liquid-crystalline phases, as has been confirmed for compounds #1 [6], #2 [16] and #3 [19]. For the *trans* isomers of compound #1 and #2 the lowest $n \rightarrow \pi^*$ transition is located at approximately 2.7 eV. For the *cis* isomers of compound #1 and #2 two low-lying $n \rightarrow \pi^*$ transitions are found around 2.65–2.75 eV in each compound. The oscillator strengths of all these transitions are in the range 0.02–0.04.

The calculated absorption and polarizability spectra of the *trans* isomers are shown in figure 3. The increased absorption accompanying the red-shift is clearly noticeable. The long-axis (x-axis) component has been compared to the sum of x-, y- and z-components (equal to three times the orientational average) in the cases of absorption (figure 3(a)) and polarizability (figure 3(b)). The results clearly show that all *trans* isomers are practically perfectly one-dimensional. A small deviation from perfect anisotropy is seen on the high-energy side of the fundamental absorption band. However, for practical purposes, all *trans* isomers can be regarded as one-dimensional in the major part of the absorption band. It is noticed that in the case of proper azobenzenes (compounds #1 and #2), both the $\pi \rightarrow \pi^*$ band as well as the $n \rightarrow \pi^*$ bands around 450 nm are completely polarized. The behaviour of the four *cis* isomers is more complicated, as shown in figures 4 and 5. For clarity we have shown the results for each compound in a separate graph. Again, by our choice of coordinate system the x-component of the absorption cross section is completely dominating in the $\pi \rightarrow \pi^*$ band. However, in the cases of compounds #1 and #2 the $n \rightarrow \pi^*$ bands are found to be significantly less polarized. From the figure it is seen that $\Sigma\sigma_i \approx z\sigma_x$ and a closer analysis of the Cartesian components reveals that $\sigma_y \approx \sigma_x$ while $\sigma_z \approx 0$. The explanation for this behaviour is that the $n \rightarrow \pi^*$ band contains two closely spaced transitions. These transitions, which are denoted $n_\pm \rightarrow \pi^*$ [15], are polarized along the x- and y-axis, respectively, but due to different selection

Table 1. Calculated parameters for *trans* and *cis* isomers of the four azocompounds shown in figure 1. In the table, E_S denotes the excitation energy of the lowest $\pi \rightarrow \pi^*$ singlet transition and f_S is the corresponding oscillator strength. In addition, E_T is the lowest triplet energy and μ_i is the ith Cartesian component of the dipole moment (1D = 3.3×10^{-30} C m).

trans isomers						
Comp. #	E_S (eV)	f_S	E_T (eV)	μ_x (D)	μ_y (D)	μ_z (D)
1	3.41	1.09	2.15	−6.54	−0.84	0.02
2	3.31	1.10	2.10	−10.4	−1.20	0.01
3	2.80	1.53	1.13	−16.0	−0.25	0.53
4	2.48	1.71	0.81	−23.9	−1.27	0.02
cis isomers						
Comp. #	E_S (eV)	f_S	E_T (eV)	μ_x (D)	μ_y (D)	μ_z (D)
1	3.73	0.33	2.64	−3.15	1.24	−0.03
2	3.56	0.29	2.58	−4.67	3.99	−0.07
3	2.61	0.50	1.29	−12.0	−3.05	1.12
4	1.89	0.23	0.89	−12.2	−0.18	−0.05

rules only the $n_+ \rightarrow \pi^*$ transition is allowed in the *trans* geometry whereas both transitions are allowed for the *cis* geometry (this difference is caused by the fact that the z- and y-directions are approximate rotational symmetry axes in the *trans* and *cis* cases, respectively). In the *cis* geometry, the two transitions carry approximately equal oscillator strength and consequently the *cis* molecule is isotropic in the (x, y)-plane. Hence, the presence of a separate $n \rightarrow \pi^*$ band is seen to lead to significant differences between the anisotropy of proper azobenzenes and pseudo-stilbenes. The results for the *cis* polarizabilities in figure 5 show a similar effect of the $n \rightarrow \pi^*$ transitions and it is found that $\alpha_{yy} \approx \alpha_{xx}$ in this band. The pseudo-stilbenes are approximately one-dimensional on the low-energy side of the $\pi \rightarrow \pi^*$ band. However, at smaller wavelengths the presence of multiple transitions makes the picture more complicated.

3. Simulations

The above results lead to the conclusion that concerning excitations in the $n \rightarrow \pi^*$ band the proper azobenzenes differ from pseudo-stilbenes in that the *cis* isomers of the former group are quasi-two-dimensional whereas those of the latter are essentially one-dimensional. In relation to optical storage experiments this difference is important since the wavelengths of the Ar-ion laser (488 nm and 514 nm), which are usually used for recording [1–9], lie in the $n \rightarrow \pi^*$ band. By using light sources of shorter wavelength, however, the more polarized $\pi \rightarrow \pi^*$ band may be utilized. As argued in the introduction, highly anisotropic chromophores are expected to lead to improved storage performance and so the $\pi \rightarrow \pi^*$ band should be preferable to the $n \rightarrow \pi^*$ band. In order to substantiate this picture we consider the rate equations for the angular distributions of *trans* and *cis* molecules. In [11, 12] we derived these equations under the simplifying assumptions that both isomers support liquid-crystalline phases with similar mean-field potentials and, furthermore, that both isomers are perfectly one-dimensional. More realistically, only the *trans* isomers are mesogenic and assuming that the reorientation of the *cis* isomers is completely random the modified rate equations for one-dimensional isomers read as

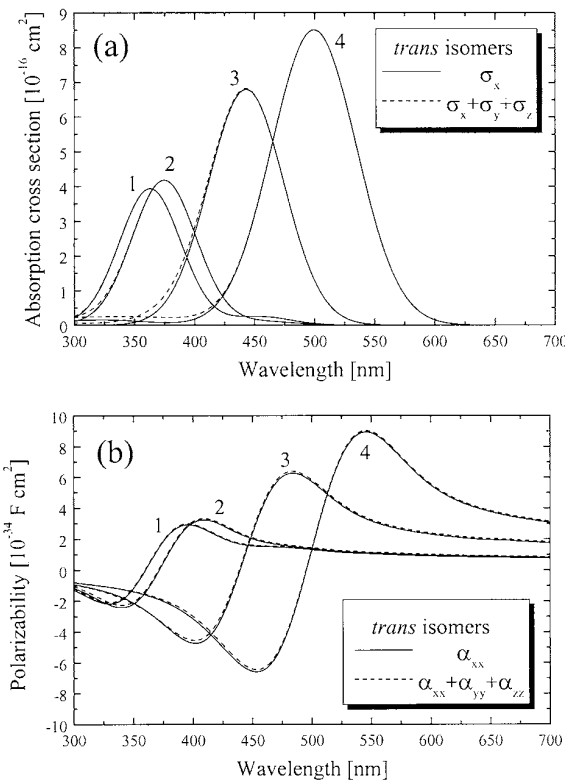

Figure 3. (*a*) Calculated *trans* absorption cross section for different compounds. The solid curves are the x-axis (long-axis) components and the dashed curves are the sum of all Cartesian components. (*b*) As figure 3(*a*) but for the polarizability.

$$\frac{\mathrm{d}}{\mathrm{d}t} f_T(\theta, \varphi) = A_{CT} I p(\theta, \varphi) \int f_C(\theta, \varphi) \cos^2\theta \, \mathrm{d}\Omega - A_{TC} I f_T(\theta, \varphi) \cos^2\theta + \frac{1}{\tau}[N_T p(\theta, \varphi) - f_T(\theta, \varphi)], \quad (1)$$

and

$$\frac{\mathrm{d}}{\mathrm{d}t} f_c(\theta,\varphi) = A_{TC} I \frac{1}{4\pi} \int f_T(\theta,\varphi)\cos^2\theta \,\mathrm{d}\Omega - A_{CT} I f_C(\theta,\varphi)\cos^2\theta + \frac{1}{\tau}\left[N_C \frac{1}{4\pi} - f_C(\theta,\varphi)\right]. \quad (2)$$

In these expressions, the polar angles (θ,φ) of a molecule are defined with respect to the polarization direction of the optical field given by (0, 0) and, hence, $\cos\theta$ is the projection of the field onto the molecular long-axis. The *trans* and *cis* distribution functions are denoted $f_T(\theta,\varphi)$ and $f_C(\theta,\varphi)$, respectively, and $p(\theta,\varphi)$ is the equilibrium distribution of the mesogenic *trans* isomers. These functions describe the properties of a particular microdomain characterized by a nematic director and an order parameter S. The angular coordinates of the director are $(\delta, 0)$ and using the Maier–Saupe [20] form of the mean-field potential, the equilibrium distribution $p(\theta,\varphi)$ is given by $p(\theta,\varphi) = A\exp\{c_0 S\cos^2\beta\}$, where A is a normalization constant, c_0 is the activation energy normalized by $k_B T$ and β is the angular separation between the direction (θ,φ) and the director, i.e. $\cos\beta = \cos\theta\cos\delta + \sin\theta\sin\delta\cos\varphi$. In addition, $A_{CT} I\cos^2\theta$ denotes the $cis \rightarrow trans$ photoisomerization rate, which is the product of the projected light intensity $I\cos^2\theta$ and $A_{CT} = (\hbar\omega)^{-1}\sigma_C\phi_{CT}$, where σ_C is the *cis* absorption cross section and ϕ_{CT} is the $cis \rightarrow trans$ isomerization quantum efficiency. Similarly, the $trans \rightarrow cis$ rate constant is $A_{TC} I\cos^2\theta$. Finally, the last terms in (1) and (2) represent the relaxation towards equilibrium with time constant τ and total *trans* and *cis* populations denoted by N_T and N_C, respectively.

The extension of the model to describe two-dimensional *cis* isomers is straightforward and essentially similar to the case of amorphous polymers described by Dumont *et al* [21]. The polar angles of the long-axis as well as the rotation of the molecule around this direction describe the orientation of a particular chromophore. We assume, however, that the average rotation around the long-axis is random and, hence, the absorption cross section averaged with respect to rotation around the long-axis is ellipsoidal. The long- and short-axis values are denoted $\sigma_{C,L}$ and $\sigma_{C,S}$, respectively. With this notation the isomerization rate is now proportional to $\sigma_{C,L}\cos^2\theta + \sigma_{C,S}\sin^2\theta = \sigma_{C,S} + (\sigma_{C,L} - \sigma_{C,S})\cos^2\theta$. It is now a simple matter to show that the modified rate equations are given by

$$\frac{\mathrm{d}}{\mathrm{d}t} f_T(\theta,\varphi) = A^I_{CT} I p(\theta,\varphi) N_C + A^A_{CT} I p(\theta,\varphi)\int f_C(\theta,\varphi)\cos^2\theta \,\mathrm{d}\Omega - A_{TC} I f_T(\theta,\varphi)\cos^2\theta + \frac{1}{\tau}[N_T p(\theta,\varphi) - f_T(\theta,\varphi)], \quad (3)$$

and

$$\frac{\mathrm{d}}{\mathrm{d}t} f_C(\theta,\varphi) = A_{TC} I \frac{1}{4\pi}\int f_T(\theta,\varphi)\cos^2\theta \,\mathrm{d}\Omega - A^A_{CT} I f_C(\theta,\varphi)\cos^2\theta - A^I_{CT} I f_C(\theta,\varphi) + \frac{1}{\tau}\left[N_C\frac{1}{4\pi} - f_C(\theta,\varphi)\right], \quad (4)$$

where $A^A_{CT} = (\hbar\omega)^{-1}(\sigma_{C,L} - \sigma_{C,S})\phi_{CT}$ and $A^I_{CT} = (\hbar\omega)^{-1}\sigma_{C,S}\phi_{CT}$ are the anisotropic and isotropic contributions to the transition rate, respectively.

For simplicity, we will only discuss the photostationary case, i.e. the steady state solution to the angular distribution functions in the presence of light. In this case it can be shown that the solutions to the above equations are given by

$$f_T(\theta,\varphi) = \left\{\frac{1-\Lambda_C}{\Lambda_T(1-\Lambda_C) + \Lambda_C(1-\Lambda_T)}\right\} \times \frac{p(\theta,\varphi)}{1+\tau A_{TC} I\cos^2\theta} \quad (5)$$

and

$$f_C(\theta,\varphi) = \left\{\frac{1-\Lambda_T}{\Lambda_T(1-\Lambda_C) + \Lambda_C(1-\Lambda_T)}\right\} \times \frac{(4\pi)^{-1}}{1+\tau A^I_{CT} I + \tau A^A_{CT} I\cos^2\theta}, \quad (6)$$

where $\Lambda_{T,C}$ are defined by

$$\Lambda_T = \int \frac{p(\theta,\varphi)}{1+\tau A_{TC} I\cos^2\theta}\,\mathrm{d}\Omega \quad (7)$$

and

$$\Lambda_C = \int \frac{(4\pi)^{-1}}{1+\tau A^I_{CT} I + \tau A^A_{CT} I\cos^2\theta}\,\mathrm{d}\Omega = \frac{1}{\sqrt{\tau A^A_{CT} I(1+\tau A^I_{CT} I)}}\tan^{-1}\sqrt{\frac{\tau A^A_{CT} I}{1+\tau A^I_{CT} I}}. \quad (8)$$

The photostationary angular distributions can be used to derive the photostationary birefringence Δn. In analogy to the *cis* absorption cross section we take the *cis* polarizability to be ellipsoidal with long- and short-axis components denoted by $\alpha_{C,L}$ and $\alpha_{C,S}$, respectively. This polarizability can be considered as the sum of an isotropic contribution $\alpha_{C,S}$ and a perfectly anisotropic contribution given by $\alpha^A_C = \alpha_{C,L} - \alpha_{C,S}$. Only the anisotropic part contributes to the birefringence and, following [11, 12], Δn can be calculated from the expression

$$\Delta n = \frac{N}{2\varepsilon_0 \bar{n}}\langle \alpha_T a_T + \alpha^A_C a_C\rangle, \quad (9)$$

where N is the density of chromophores, $\bar{n}$ is the average index (taken as its unperturbed value) and the coefficients α_T and a_C are given by $a_X = \int f_X(\theta,\varphi)P_2(\cos\theta)\,\mathrm{d}\Omega$ with $X = T, C$. In addition, the angular brackets signify averaging over all microdomains.

A convenient way of comparing one- and two-dimensional chromophores is by introducing a 'molecular *cis* ellipticity' f defined by

$$\sigma_{C,L} = \sigma_C(1-2f), \qquad \sigma_{C,S} = \sigma_C f. \quad (10)$$

Note that this definition leaves the average $(\sigma_{C,L} + 2\sigma_{C,S})/3 = \sigma_C/3$ a constant while f is varied. In terms of the ellipticity we find $A^A_{CT} = A_{CT}(1-3f)$ and $A^I_{CT} = A_{CT} f$ with $A_{CT} = (\hbar\omega)^{-1}\sigma_C\phi_{CT}$. Naturally, for a particular chromophore the ellipticity is a wavelength-dependent function. By inspection of figure 4 we find that the $n \rightarrow \pi^*$ band of the proper azobenzenes is characterized by $f \approx 0.25$ while $f \approx 0$ for

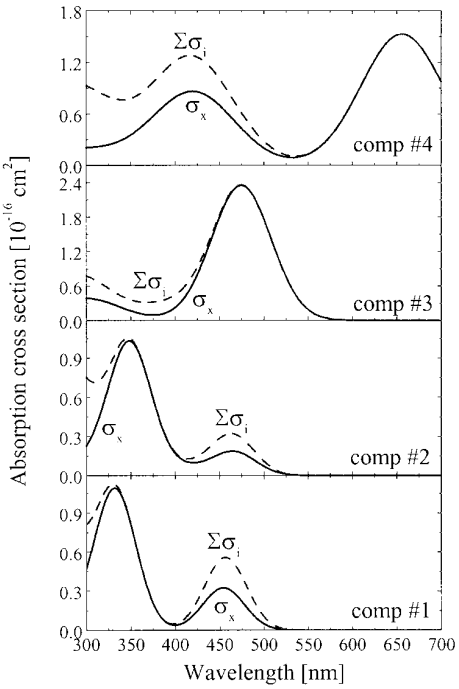

Figure 4. Calculated *cis* absorption cross section for different compounds. Solid and dashed curves are long-axis and summed components, respectively. The bands around 450 nm in compounds #1 and #2 are $n \rightarrow \pi^*$ bands and all others are $\pi \rightarrow \pi^*$ bands.

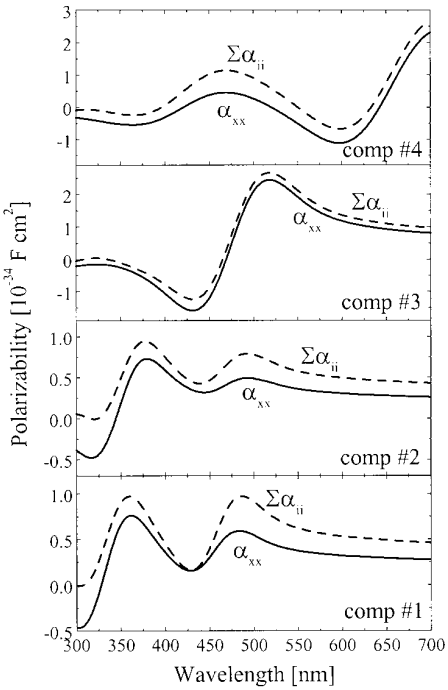

Figure 5. As figure (4) but for the components of the *cis* polarizability.

the pseudo-stilbenes. The influence of the ellipticity is most clearly illustrated by focusing on a single model compound for which f can be varied while keeping all other parameters fixed. Assuming a typical density of $N = 10^{21}$ cm^{-3} we will take $\sigma_T = \sigma_C = 3 \times 10^{-18}$ cm^2 for this model compound since this corresponds to a reasonable penetration depth of 10 μm. From figure 3 it is seen that a *trans* absorption cross section of this magnitude can always be realized by a proper choice of wavelength. The assumed equality between σ_T and σ_C is only approximately valid, however. Furthermore, we will use $\phi_{TC} = 0.1$ and $\phi_{CT} = 0.4$ [14] and $\hbar\omega = 2.54$ eV (absorption wavelength $\lambda_{abs} = 488$ nm). In the long-wavelength range the components of the *cis* polarizability of pseudo-stilbenes and proper azobenzenes yield ellipticities of approximately 0.05 and 0.20, respectively (see figure 5). For use in the present simple simulation, however, we will assume identical ellipticities for polarizability and absorption and so the components of the polarizability are taken as

$$\alpha_{C,L} = \alpha_C(1 - 2f), \qquad \alpha_{C,S} = \alpha_C f, \qquad (11)$$

and so $\alpha_C^A = \alpha_C(1 - 3f)$. The polarizability of the perfectly anisotropic *trans* isomers is taken as $\alpha_T = 2\alpha_C$. For the actual calculations we will use the average of the $\lambda = 700$ nm values for the four chromophores which is $\alpha_T \approx 1.6 \times 10^{-34}$ Fcm^2. With this value we find $N\alpha_T/(2\varepsilon_0\overline{n}) \approx 0.6$. Finally, we take as a typical value $S = 0.5$ and for the remaining macroscopic parameters we adopt the values of [12], i.e. $c_0 = 6.8$ and relaxation time and threshold intensity of domain rotation as $\tau = 10$ s and 135 mW cm^{-2}, respectively.

The results of the simulations are presented in figures 6(a) and (b). The birefringence curves have been calculated for $f = 0.0, 0.1, 0.2$ and 0.3 in order to cover the relevant range. A substantial decrease of the birefringence with increasing molecular ellipticity is noticed, especially for low and moderate intensity. The relative difference between the curves labelled $f = 0.0$ and $f = 0.3$ varies from ∼25% at low intensity to approximately 5% at an intensity of 400 mW cm^{-2}. At even higher intensities the difference decreases further since the lack of *cis* anisotropy is compensated by an increased *trans* population. The reason for this effect is that *cis* isomers are continuously excited irrespective of their orientation due to the isotropic contribution to the absorption cross section. Conversely, *trans* isomers may completely escape absorption by being oriented in the plane perpendicular to the optical field. Hence, at very high intensities the polymer approaches a state characterized by a *trans* population of 100% and all chromophores contained in a single plane. In fact, at these high intensities the curves shown in figure 6(a) will cross leading to increasing birefringence with molecular ellipticity. In the more relevant range shown in figure 6(a); however, the results demonstrate that the storage performance of perfectly anisotropic molecules is superior to that of ellipsoidal ones. It should be kept in mind that this conclusion is based on an analysis of a fictitious model compound for which the ellipticity is varied while all other parameters are fixed. Hence, the results should only be regarded as an estimate of the storage performance of actual chromophores with different degrees of anisotropy. For the four different compounds considered in this work, simulations based on the actual parameters are shown in figure 6(b). Again, to ensure a reasonable penetration depth we have chosen $\sigma_T = 3 \times 10^{-18}$ cm^2, i.e. the four simulations are done at four different wavelengths (506, 499, 546 and 618 nm) in order to satisfy this condition. The improved performance

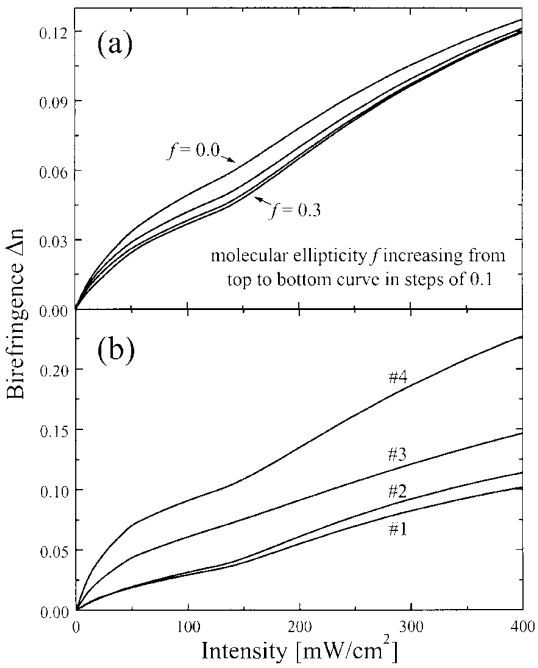

Figure 6. Simulated intensity dependence of the photostationary birefringence. (*a*) The four curves are calculated for a fictitious model compound using four different values of the *cis* ellipticity f while keeping all other parameters fixed. (*b*) Simulations based on the actual parameters characterizing the four different compounds.

of compounds #3 and #4 is clearly visible in these curves. The improvement, however, is due to a combination of larger polarizability as well as higher degree of anisotropy. Hence, the differences between curves is not only due to differences in molecular ellipticity.

4. Summary

In this paper we have applied molecular quantum calculations to study the effects of substituents on the storage performance of azobenzene polymers with potential use for reversible optical data storage. Long-term optical storage in these materials is based on reorientation of the azobenzene chromophores in a linearly polarized optical field. The process requires different absorption probabilities for molecules oriented parallel and perpendicular to the polarization direction and for this reason we have focused on calculations of molecular anisotropy. The *trans* isomers of the chromophores are found to be essentially one-dimensional in all cases. The degree of anisotropy of the *cis* isomers, however, is highly dependent on the relative location of the $n \rightarrow \pi^*$ and $\pi \rightarrow \pi^*$ absorption bands. In the case of overlapping bands (so-called pseudo-stilbenes) the *cis* isomers are approximately one-dimensional but with well-separated bands (proper azobenzenes) the $n \rightarrow \pi^*$ band is much less polarized. In order to compare the storage performance in the two cases we have presented simulations of the photoinduced reorientation in a liquid-crystalline polymer containing a model chromophore for which the degree of anisotropy is varied. When the degree of anisotropy is gradually decreased it is found that the birefringence may be reduced by as much as 25% using realistic parameters.

References

[1] Todorov T, Nikolova L and Tomova T 1984 *Appl. Opt.* **23** 4309
[2] Eich M, Wendorff J H, Reck B and Ringsdorf H 1987 *Macromol. Chem. Rapid Commun.* **8** 59
[3] Natansohn A, Rochon P, Gosselin J and Xie S 1992 *Macromolecules* **25** 2268
[4] Rochon P, Gosselin J, Natansohn A and Xie S 1992 *Appl. Phys. Lett.* **60** 4
[5] Hvilsted S, Andruzzi F and Ramanujam P S 1992 *Opt. Lett.* **17** 1234
[6] Hvilsted S, Andruzzi F, Kulinna C, Siesler H W and Ramanujam P S 1995 *Macromolecules* **28** 2172
[7] Eich M and Wendorff J 1990 *J. Opt. Soc. Am.* B **7** 1428
[8] Holme N C R, Ramanujam P S and Hvilsted S 1996 *Opt. Lett.* **21** 902
[9] Berg R H, Hvilsted S and Ramanujam P S 1996 *Nature* **383** 505
[10] Sekkat Z and Dumont M 1993 *Synth. Met.* **54** 373
[11] Pedersen T G and Johansen P M 1997 *Phys. Rev. Lett.* **79** 2470
[12] Pedersen T G, Johansen P M, Holme N C R, Ramanujam P S and Hvilsted S 1998 *J. Opt. Soc. Am.* B **15** 1120
[13] Lucchetti L, Simoni F and Reznikov Y 1999 *Opt. Lett.* **24** 1062
[14] Rau H 1990 *Photochromism Molecules and Systems* ed H Dürr and H Bouas-Laurent (Amsterdam: Elsevier)
[15] Pedersen T G, Ramanujam P S, Johansen P M and Hvilsted S 1998 *J. Opt. Soc. Am.* B **15** 2721
[16] Pedersen M 1997 *PhD Dissertation* Risø National Laboratory, Denmark
[17] Griffiths J 1982 *Dyes Pigm.* **3** 211
[18] Shuto Y 1996 *Int. J. Quantum Chem.* **58** 407
[19] Koch A T H, Warner M, Fridrikh S V, Toussaere E, Zyss J, Schwarzwälder C E, Tajbakhsh A R, Moratti S C and Friend R H *Optoelectronics Group, Cavendish Laboratory, Cambridge* Private communication
[20] Maier W and Saupe A 1959 *Z. Naturf.* a **14** 882
[21] Dumont M, Froc G and Hosotte S 1995 *Nonlinear Opt.* **9** 327